Adv. Space Res. Vol.5, No.7, pp.69-72, 1985
Printed in Great Britain.

0273-1177/85 $0.00 + .50

AN EXPERIMENTAL AND EMPIRICAL MODEL OF ELECTRON TEMPERATURE FOR ALTITUDES OF 500 TO 1000 km AND FOR A HIGH SOLAR ACTIVITY PERIOD

J. Šmilauer* and V. V. Afonin**

*Geophysical Institute of Czechoslovakian Academy of Sciences, Prague, Bočni II, 14131, Czechoslovakia
**Space Research Institute of the U.S.S.R. Academy of Sciences, Moscow, Profsoyuznaya 84/32, 117810, U.S.S.R.

ABSTRACT

On the basis of systematic electron temperature measurements onboard the Interkosmos-19 satellite, an experimental global model of electron temperature T_e has been constructed; namely, a set of samples representing 1o intervals of measured T_e, accompanied by values of the geographic longitude, solar zenith angle, season of the year, Covington index, Dst and Kp, grouped according to the invariant latitude, geomagnetic time and altitude. On the basis of the experimental model, the coefficients of the empirical models for the summer and winter seasons, for geophysically quiet conditions, and for heights of 52o, 6oo, 92o and 1ooo km are calculated. For heights of 68o, 76o and 84o km with fewer data available, the coefficients are provisional.

INTROLUCTION

A knowledge of electron temperature behaviour in the ionosphere is of considerable importance both for studies of specific geophysical phenomena (e.g. ionosphere-magnetosphere coupling) and for model calculations in a number of applications. Therefore, two related tasks have been undertaken: 1) Construction of an experimental model to facilitate a study of the influence of selected geophysical parameters on the behaviour of T_e, and yielding data for concrete geophysical situations; 2) Formation of a mathematical representation of the model for very general situations.

Quite undisputed is the significance of an electron temperature model, the implicit parameter of which is the electron density N_e. In such a model, the T_e-changes caused by N_e-changes are compensated to a considerable extent, and this emphasizes the effects of heat energy sources, especially of the non-local ones. Therefore, a model of the product $T_e \times \log N_e$ has been made in parallel with the T_e-model. Since sufficient data are not yet available, the $T_e \times \log N_e$ model is not presented here.

THE DATA EMPLOYED AND THEIR ASSORTMENT

The Interkosmos-19 satellite (1979-o2oA, perigee and apogee heights 5oo and 1ooo km respectively, orbital inclination 74°) carried the KM-3 equipment to measure the electron temperature and the energy distribution of thermal electrons /1/. The period of the ascending node variations was about 125 days, and of the variation of the perigee argument about 167 days. The measured data were stored in an on-board memory, and the following two operational regimes are important for our purposes: 1) A long-term record of about 1o24 min duration with a step of o.64 s for individual T_e-measurements; 2) A short-term record of about 128 min duration, with the step of about o.o8 s. Since the apparatus for the measurement of electron density failed, it proved necessary to try to determine N_e from the data obtained by measurements of the energy distribution. This distribution was measured in much longer steps, namely every 168 s in the long-term operational regime, and every 24 s in the short-term one. During the satellite's active period (from 28 February 1979 to 1 March 1981, with several switch-off pauses), a considerable amount of data on the global T_e-distribution was transmitted from the satellite and evaluated, but there were fewer simultaneous T_e- and N_e-measurements. This paper is based on 185 long-term records representing measurements from about 16oo complete satellite revolutions.

The invariant latitude INVLAT, geomagnetic local time TGEM and latitude ALT were used as principal variables of the model, the INVLAT for southern latitudes being taken as negative. On the basis of about 6o long-term records, a comparison between the INVLAT and the parameter MODIP /2/ was made; the grouping according to INVLAT showed a smaller scatter of data. This is probably due to the greater heights (as compared with /2/) at which the photoelectron fluxes play a significant role, as well as the influences of the plasmaspheric reservoir, both of which are closely connected with the structure of the magnetic lines of force. The T_e-values have been averaged; one sample corresponds to a mean value over about 1o s (16 measurements for the long-term operational regime). The data were smoothed using regression analysis, and by an iterative exclusion of the points with the greatest deviation until the ratio (mean value/RMS)> 1oo was attained. Every point of the model consists of the temperature value and the values of all ariables and parameters as given in Table 1, which includes range, step and the number of levels. The levels of INVLAT and TGEM are expressed by the serial number of one of 2916 records stored in the disc memory; all other quantities are contained in three 16-bit words. An important feature of the experimental model is the possibility of selecting a wanted data record with an accuracy better than one day.

THE EXPERIMENTAL AND EMPIRICAL MODEL

After putting in about 185 long-term records, the experimental T_e-model contains about $9 \cdot 1o^5$ points; the content of the T_e x log N_e-model is less by a factor of 1o. An idea of the homogeneity and representativeness of the model can be obtained from histograms of the individual parameters (Figure 1). The histograms of INVLAT and ALT are essentially determined by the orbit, and they show that the model is valid for INVLAT in the range of about $\pm$ 75°, and for heights of 5oo to 1o1o km, with preferred heights around 53o and 99o km. The time distribution of data is characterized, one the one hand, by histograms TGEM and GLON showing a relatively homogeneous distribution within short time-periods, and on the other, by the seasonal histogram which shows a less favourable contribution of the winter season as compared with the summer one. From the histogram of the Covington index, it can be seen that all the data used fall into the interval CI > 135, the mean value being about 185, and the most probable values about 189 and 155. Finally, it follows from histograms of Kp and Dst that roughly 6.5% of the data were obtained in disturbed periods (Dst < -45 nT, Kp > 4).

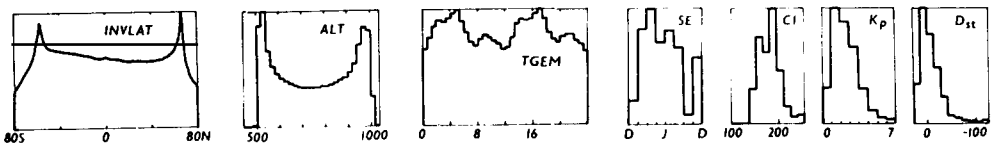

Fig. 1. Histograms of the parameters of our experimental T_e model.

TABLE 1 Parameters of our T_e Model

Parameter	Range	Step	Number of steps
TE	8oo .. 1o23o	1o K	1o23
INVLAT	-81 .. 81	2°	81
TGEM	0 .. 144o	4o min	36
ALT	4oo .. 1o4o	2o km	32
GLON	0 .. 36o	6°	6o
CHI	< 55 55 .. 115 >115	1o°	8
SE	0 .. 365	46 d	8
DST	3o .. -21o	15 nT	16
KP	0 .. 7	1	8
CI	6o .. 3oo	log	16
IWR	1 .. 511	1	511

SE, season, begins with the winter solstice; IWR, number of the record.

The mathematical representation of the experimental model obtained has been chosen remembering that the data originate from a satellite with an orbit of high inclination and low excentricity. Partially, this was already respected by a higher latitude resolution (in contrast to the TGEM-resolution); a further consequence is the possibility of constructing level models for altitude intervals. The possibility of determining the dependence on height is considerably restricted. The empirical models have been calculated for the following altitudes: 520, 600, 680, 760, 840, 920 and 1000 km; the individual models involve data from the range of ± 40 km. For the description of the T_e distribution, orthogonal zonal functions were used up to the 8th order. To ensure comparability of the results with the data from the AE-C, ISIS-1 and ISIS-2 satellites, normalization was applied, and an expansion of $\log_{10}(T_e)$ /3/ was made:

$$\log_{10}T_e = CC_o^o + \sum_{n=1}^{8}\left\{CC_n^o\, P_n^o(\cos\vartheta) + \sum_{m=1}^{n}\left[(CC_n^m\cos(m\varphi) + CS_n^m\sin(m\varphi)\right] P_n^m(\cos\vartheta)\right\} \quad (1)$$

Since the experimental data cover mainly uniformly the whole range of INVLAT and TGEM, the coefficients of Equation (1) were calculated by numerical integration to a first approximation, after insertion of missing values. Later, the coefficients were recalculated by the method of least squares assuming conjugate gradients. The data were given weights corresponding to the number of points within the interval considered. The weight for 3 to 10 values is 1, for 11 to 30 values it is 2 and for more than 30 values it is 4. The weight given to temperature values was doubled for $|INVLAT| < 48^o$.

RESULTS AND DISCUSSION

The coefficients for our solar maximum electron temperature models at heights 520, 600, 920 and 1000 km for summer (SA) and winter (WA) can be found in the Annex. The global T_e-distribution after model 520 SA is shown in Figure 2, but such graphs are available for all models. The RMS deviations from the model were also studied. An enhanced scatter occurs in the auroral regions, in the dawn sector and in the afternoon sector of the equatorial region. The scatter of values in the dawn sector is obviously caused both by differences in TGEM and SLT, and by changes of CHI in the course of the season; the equatorial scatter (heights 500 to 600 km) is connected with an equatorial temperature anomaly which is often observed in regions of about ± 15° around the equator.

Finally, a comparison of our model with those of /3/ has been made. As an example, the diurnal T_e-variation is given for 40° northern invariant latitude (Figure 3). In spite of quite different solar activity, very similar patterns appear; owing to the enhanced solar activity, a certain increase of

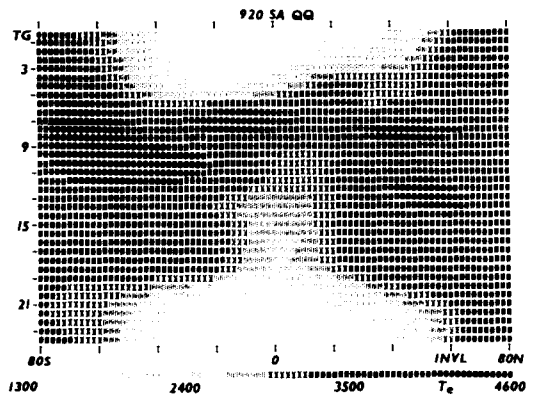

Fig. 2. Statistical average distribution of T_e by local hour (ordinate) and invariant latitude (abscissa). Temperature scale below.

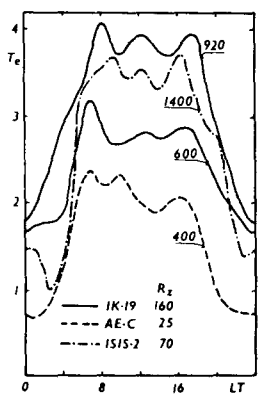

Fig. 3. Diurnal variation of T_e at 40°N invariant latitude after Interkosmos 19 (full lines) and AE-C, ISIS-2 /3/ (broken).

daytime temperatures is seen with Interkosmos-19, as well as a considerable enhancement of nighttime temperatures, obviously as result of the well-known increase in neutral temperature. In the equatorial region, the equatorial anomaly is striking at the height of 52o km (between about 12 and 18 MLT).

In the near future, it will be possible to complete the experimental model using the data from about 24o short-term records; as a result, a slight increase of the data volume in the T_e-model will be achieved (by about $3 \cdot 1o^5$ points), and also a substantial increase in the model for $Te \times \log N_e$ (by about $2 \cdot 1o^5$ points).

The models represent an addition to the previous models (AE-C, ISIS-1, ISIS-2) involving the outer ionosphere region and the period of high solar activity. However, all these models reflect rather a latitude and local time behaviour of T_e, and they obviously cannot be employed for obtaining the height profiles. For the construction of a three-dimensional model, the simultaneous employment of satellite and incoherent scatter data seems essential.

REFERENCES

1. K. Kubat, Ya. Klas, Ya. Shmilauer and V.V. Afonin, Instrument KM-3 for measurement of electron temperature and the velocity distribution of thermal electrons (in Russian), in: Apparatura dlya issledovaniya vneshnei ionosfery (Apparatus for the study of the outer ionosphere), IZMIRAN Moscow 198o, p. 12o.

2. H. Thiemann and K. Rawer, Empirical electron temperature model for the daytime ionosphere deduced from AEROS-B, Preprint (1982)

3. L.H. Brace and R.F. Theis, Global empirical models of ionospheric electron temperature in the upper F-region and plasmasphere based on in-situ measurements of Atmosphere Explorer-C, ISIS-1 and ISIS-2 satellites, J. Atmos. Terr. Phys. 43, 1317 (1981)